



Strong exciton photon coupling and its polarization dependence in a metal mirror microcavity with oriented PIC J aggregates

著者	Oda Masaru, Hirata Kazuyuki, Inoue Tokiko, Obara Yuki, Fujimura Tomoko, Tani Toshiro
journal or publication title	Physica Status Solidi C
volume	6
number	1
page range	288-291
year	2009-01
URL	http://hdl.handle.net/10228/00006905

doi: [info:doi/10.1002/pssc.200879879](https://doi.org/10.1002/pssc.200879879)

Strong exciton-photon coupling and its polarization dependence in a metal-mirror microcavity with oriented PIC J-aggregates

Masaru Oda^{*1,2}, Kazuyuki Hirata², Tokiko Inoue², Yuki Obara², Tomoko Fujimura², and Toshiro Tani^{1,2}

¹ Strategic Research Initiative for Future Nano-Science and Technology, Tokyo University of Agriculture and Technology, Naka-cho 2-24-16, Kogane-i, Tokyo 184-8588, Japan

² Department of Applied Physics, Tokyo University of Agriculture and Technology, Naka-cho 2-24-16, Kogane-i, Tokyo 184-8588, Japan

Received 23 August 2007, revised 12 October 2007, accepted *zzz*
Published online *zzz*

PACS 71.36.+c, 71.35.Cc, 73.40.Sx, 78.66.Qn, 78.67.Lt, 78.67.-n

* Corresponding author: e-mail odamasa@cc.tuat.ac.jp, Phone: +81 42 388 7423, Fax: +81 42 385 6255

We present a study of strong exciton-photon coupling and its dependence on incident light polarization in a metal-metal mirror microcavity containing PIC J-aggregates. Rabi-splitting energies between upper and lower polariton branches are estimated as 94 meV and 69 meV for s- and p-polarized incident light, respectively. These large values are due to large oscillator strength of Frenkel excitons in the PIC J-aggregates and strong confinement of light attributed to the metallic microcavity as well. As for the effective thickness of the active layer for s-polarized light, a good agreement is obtained between $L_{eff}^{fit} = 201$ nm deduced from the experimental data and $L_{eff}^{calc} = 207$ nm calculated from the summation of the measured thickness of active layer with the estimated penetration depths into silver mirrors. We also discuss the difference in the polarization dependences of Rabi-splitting energy, quantitatively. It is concluded that the polarization dependence is mainly due to an alignment of the J-aggregates in the active layer and is not affected so much by anisotropy of the penetration depths into the silver mirrors.

Copyright will be provided by the publisher

1 Introduction Strong light-matter coupling in semiconductor microcavities has attracted much attention due to fundamental physical interest [1] and possible applications for low-threshold optical devices [2]. Specifically, organic semiconductor microcavities [3-5] are of interest because they have the ability to achieve strong coupling at room temperature due mostly to large oscillator strength of Frenkel excitons in the organic materials.

The coupling strength under weak light irradiation is characterised by vacuum Rabi-splitting energy. The large oscillator strength of the organic materials enables us to observe vacuum Rabi-splitting even in low-Q planar microcavities. Recently, enhancement of the Rabi-splitting of a factor of 2.3 was observed in a low Q metal-metal microcavity compared with that in a distributed Bragg reflector (DBR)-metal hybrid microcavity. Penetration depth of light into metal mirror is much shorter than that of DBR mirror due to a difference of their reflection principles. So the strong confinement of light by metallic mirror leads to

the larger Rabi-splitting [6]. It seems quite interesting that strong coupling achieved simply by the metallic cavity works effectively; however, details of the optical properties have not been sufficiently investigated.

In this paper, we present a synthesis of the metallic mirror microcavity containing PIC J-aggregates and its performance of light-matter coupling with its polarization dependence of incident light. Large Rabi-splitting and its strong polarization dependence will be described quantitatively by considering both the specific confinement due to metallic microcavity and effects arising from a macroscopic alignment of J-aggregates.

2.1 Samples As the organic semiconductor in the planar metal-mirror microcavity, we use J-aggregates of 1,1'-diethyl-2,2'-cyanine chloride (PIC-Cl, Hayashibara Biochemical Laboratories Inc.) of which the chemical structure is shown in the inset of Fig.1(a). The J-aggregates are prepared in the following way [7].

Copyright line will be provided by the publisher

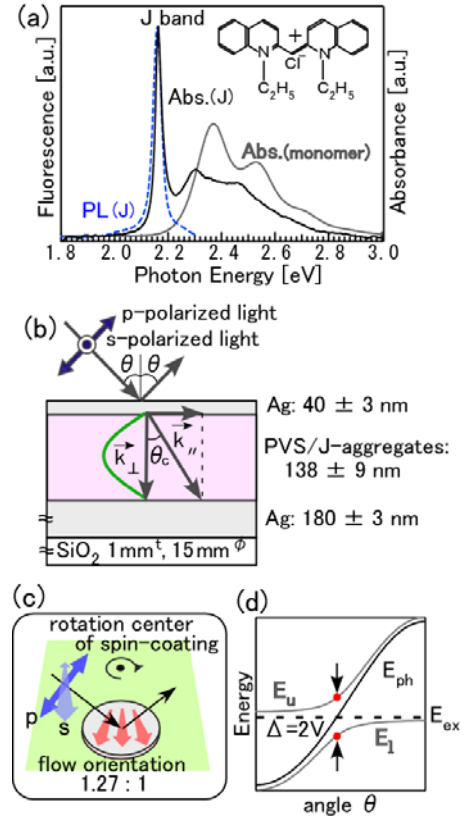
1 First, aqueous solution of potassium polyvinyl sulfate
 2 (PVS-K) is prepared by dissolving 155 mg of PVS (Wako
 3 Pure Chemical Ind.) in 3.6 mL of distilled water (4.3 wt%)
 4 at 90 °C. Separately, 3.62 mg of the PIC dye is dissolved in
 5 1 mL of methanol (10 mM). Then, 0.4 mL of this PIC
 6 methanol solution is injected into the PVS aqueous
 7 solution kept at 90 °C. The black and gray lines in Fig. 1(a)
 8 show absorption spectra of the so prepared PIC J-
 9 aggregates in the aqueous solution and of PIC monomers
 10 in the methanol solution at room temperature, respectively.
 11 A strong and narrow band with a FWHM less than 35 meV
 12 appears at 2.16 eV, which ensures that Frenkel type
 13 excitons are formed due to an aggregation of the PIC
 14 molecules (J-aggregates). The broken line in Fig. 1(a)
 15 shows a photoluminescence spectrum of the J-aggregates.
 16 As expected, Stokes shift between absorption and
 17 photoluminescence maxima is negligible. Sharp absorption
 18 and photoluminescence bands are referred as J-band. The
 19 absorption and photoluminescence transition dipoles of the
 20 J-band are oriented along the long axis of PIC J-aggregates.
 21 These specific optical properties of the J-band can be basi-
 22 cally described based on the model that PIC molecules
 23 form a one-dimensional chain structure. Although, more
 24 developed structure, such as one-dimensional zigzag chain
 25 structure [8] or helical structure [9], has been proposed to
 26 describe detailed optical properties of the J-band and also
 27 of higher absorption bands at 2.30 and 2.46 eV, the one-
 28 dimensional model without fine structure is simple and ex-
 29 tremely useful as far as explaining basic properties of the
 30 J-band. Thus, we adopt here the simple one-dimensional
 31 model.

32
 33 The microcavity structure shown in Fig. 1(b) was fab-
 34 ricated as follows. A silver mirror is deposited onto a silica
 35 glass substrate (thickness: 1 mm, diameter: 15 mm) by
 36 thermal evaporation, and then an active layer of a PVS film
 37 containing the J-aggregates is formed by spin-coating. To
 38 form a flat layer, the glass substrate is placed at off-
 39 centered position from rotation axis of the spin-coating. It
 40 also provides flow alignment of the J-aggregates. The ratio
 41 of radial orientation to its perpendicular one was estimated
 42 as 1.27 (Fig. 1(c)) from a polarization measurement of
 43 photoluminescence intensity of the J-band. Finally, a sec-
 44 ond silver film is deposited onto the active layer by ther-
 45 mal evaporation. Thicknesses of the layers are 180 ± 3 nm,
 46 138 ± 9 nm and 40 ± 3 nm, respectively.

47
 48 **2.2 Cavity-polaritons** In a planar microcavity (Fig.
 49 1(b)), the energy of photon mode E_{ph} is given by

$$50 \quad E_{ph} = \frac{\hbar c}{n} |\vec{k}| = \frac{\hbar c}{n} \sqrt{|\vec{k}_\perp|^2 + |\vec{k}_\parallel|^2}, \quad (1)$$

51
 52 where \hbar , c and n are the Plank's constant divided by 2π ,
 53 the speed of light, the refractive index of the material with-
 54 in the cavity. \vec{k} , \vec{k}_\perp , \vec{k}_\parallel are wave vector of light in the



55
 56
 57
Figure 1 (a) The absorption spectra of PIC dye monomers in methanol solution (gray line) and PIC J-aggregates (black line) dispersed in a PVS matrix at RT. Broken line shows photoluminescence spectrum of the J-aggregates at room temperature. The inset shows the chemical structure of the PIC dye molecule. (b) Schematic diagram of the microcavity structure. The thicknesses of the layers were measured with a mechanical profile-meter (Veeco; Dectak II). (c) Schematic diagram showing the flow orientation due to spin-coating and the measurement configuration of polarization dependence of reflectivity. (d) Dispersion relation of cavity-polaritons (gray lines).

cavity, and its perpendicular and parallel components. Especially in the microcavity designed for $\lambda/2$ mode,

$$E_{ph}(\theta) = \frac{\hbar c}{n} \sqrt{(\pi/L)^2 + |\vec{k}_\parallel|^2} = E_0 \left\{ 1 - \left(\frac{\sin \theta}{n} \right)^2 \right\}^{-\frac{1}{2}}, \quad (2)$$

where L , E_0 and θ are the cavity length, the photon energy at angle $\theta = 0$ (normal incidence) and the external angle, respectively [10].

Here we adopt a model that the states in the microcavity are regarded as a coupled oscillator consisting of exciton and photon modes [1]. The coupled oscillator is described with the matrix equation by

$$\begin{pmatrix} E_{ph}(\theta) - E_{u,l} & V \\ V & E_{ex} - E_{u,l} \end{pmatrix} \begin{pmatrix} \alpha \\ \beta \end{pmatrix} = 0, \quad (3)$$

where $E_{u,l}$ is the energy of upper and lower cavity polaritons, respectively, and E_{ex} is the exciton energy ($E_{ex} = 2.16$ eV). V is the interaction energy between the photon and exciton. α and β are the coefficients of linear combination of the bare photon and exciton states. By diagonalizing the coefficient matrix, $E_{u,l}$ is given as a function of angle θ by

$$E_{u,l}(\theta) = \frac{E_{ph}(\theta) + E_{ex}}{2} \pm \frac{1}{2} \sqrt{(E_{ph}(\theta) - E_{ex})^2 + (2V)^2}. \quad (4)$$

Thus the scanning of θ around the exciton energy enables us to map out the dispersion relation for the cavity polaritons (Fig. 1(d)).

2.3 Measurements We measured angle dependences of reflection spectra of the microcavity. Dispersion relation of the upper and lower polaritons can be mapped out by plotting two dip energies observed in the reflection spectra. The vacuum Rabi splitting defined as $\Delta \equiv 2V$ was estimated from the best fittings to the data with Eq. (4).

The reflection spectra were measured by using both s-polarized incident light (perpendicular to the plane of incidence) and p-polarized incident light (parallel to the plane of incidence). Fig. 1(b) shows schematic diagram of the experimental setup. The microcavity was placed so that the flow orientation of the J-aggregates, i.e. radial direction of the spin-coating as shown in Fig 1(c), is aligned parallel with s-polarized incident light. All measurements were performed at room temperatures.

3 Results and Discussion Figures 2(a) and 2(b) show the reflection spectra of the microcavity for s- and p-polarized light, respectively, as a function of different incident angles. The vertical broken line is the peak absorption energy due to Frenkel excitons in the PIC J-aggregates.

Crosses in Fig. 2(c) are the dip energies of the reflection spectra for s-polarized incident light in Fig. 2(a), indicating the dispersion relation of the upper and lower polaritons for s-polarized light. Large Rabi-splitting of 94 meV is observed at the resonance angle $\theta^{res} = 23^\circ$. Refractive index n and cavity length L are estimated as 1.48 ± 0.1 and 201 nm, respectively, by fitting eq. (4) to the experimental data. Excellent fitting is obtained for s-polarized light. In practice, the n and L depend on penetration depth of light into the mirrors [1], thus we denote the fitted values as n_{eff}^{fit} and L_{eff}^{fit} . The obtained n_{eff}^{fit} is sufficiently equal to that of PVS polymer ($n_{PVS} = 1.49$) which used as the main matrix of the active layer.

Here, we consider a penetration effect of light into silver mirror as follows. First, we calculated a phase lag $\Delta\phi$ from π when light is reflected by the silver mirror at the resonance angle, and then penetration length is evaluated by $\Delta\phi \cdot \lambda / 2\pi$. Penetration depth along perpendicular direction for the planar microcavity (Fig. 2 (d)) is calculated by multiplication of the penetration length by $\cos\theta_c^{res}$, approximately. Here, the resonance angle in the active lay-

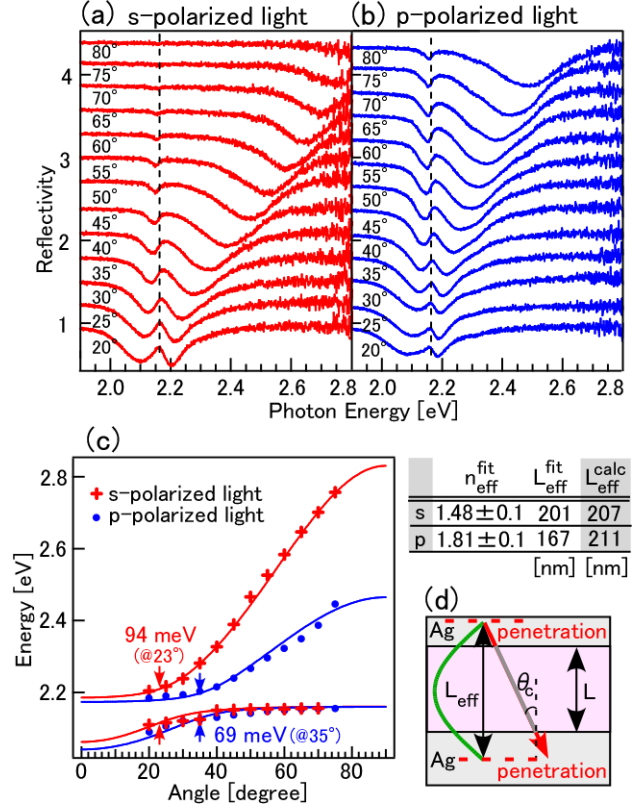


Figure 2 (a), (b) Reflectivity of the microcavity as a function of viewing angle for s- and p-polarized incident light at room temperature, respectively. Viewing angles corresponding to the individual spectra are indicated on the left side. The absorption peak energy of the J-aggregates (J-band energy) is indicated by vertical broken lines. (c) Angular dependent energy dispersion of the two cavity polariton branches for s-polarized (crosses) and p-polarized (circles) incident light, respectively. The solid lines are the best fittings to the data using the simple two-level model described by the Eq. (4). n_{eff}^{fit} and L_{eff}^{fit} shown in the table are the values obtained by the fittings. L_{eff}^{calc} is the calculated value by the model considering a penetration depth in the vertical direction. (see text for details). (d) Schematic diagram describing the penetration depth and the effective thickness L_{eff} .

er θ_c^{res} is calculated by $\sin^{-1}(n_{PVS} \sin\theta^{res})$ according to Snell's law.

The penetration depths for upper and lower mirrors are estimated as 35 nm and 34 nm, respectively, and are one order of magnitude shorter than those of DBR mirrors [6]. For s-polarized light, the agreement between $L_{eff}^{fit} = 201$ nm and $L_{eff}^{calc} = 207$ nm, summation of the measured thickness of the active layer with the calculated penetration depths, is fairly nice. Rabi-splitting of planar microcavity is inversely proportion to the square-root of cavity length [1]. Thus, we conclude the large Rabi-splitting arises from not only large oscillator strength of the PIC J-aggregates, but also strong confinement of light in the metallic microcavity.

Next, we consider the dispersion relation of polaritons for p-polarized light. Circles in Fig. 2(c) are the dip energies of the reflection spectra for p-polarized light shown in Fig. 2(b). Rabi-splitting of 69 meV is observed at the resonance angle of 35°. As for the observed strong dependence of the Rabi-splitting energy on polarization, it will be described later. $n_{\text{eff}}^{\text{fit}}$ and $L_{\text{eff}}^{\text{fit}}$ are estimated as 1.81 ± 0.1 and 167 nm, respectively. The value of $n_{\text{eff}}^{\text{fit}}$ for p-polarized light is much larger than that of PVS polymer. As shown in Fig. 1(b), s-polarized light has only in-plane electric field, whereas p-polarized light has both in-plane and out-of-plane components. For the moment, this out-of-plane component can cause the enhancement of effective refractive index in the metallic microcavity. Further investigation is surely inevitable to make clear the origin of the large value.

The fitted and calculated effective cavity lengths are $L_{\text{eff}}^{\text{fit}} = 167$ nm and $L_{\text{eff}}^{\text{calc}} = 211$ nm, respectively. In this case the agreement is not so good as in the case of s-polarization. The $L_{\text{eff}}^{\text{fit}}$ is obtained from the fitting parameter E_0 (cf. eq (2)), i.e. the energy at 0°, but it seems that the fitting curve for p-polarized light at smaller angles (lower polariton branch at Fig. 2(c)) is not exactly on the data. To discuss the details of the $n_{\text{eff}}^{\text{fit}}$ and $L_{\text{eff}}^{\text{fit}}$ for p-polarized light, it is necessary to improve the accuracy of the data at low incident angles.

Finally, we discuss the strong polarization dependence of the Rabi-splitting. Such strong dependence is not observed in microcavities containing semiconductor materials [11]. We consider first the effect which arises from alignment of the J-aggregates. The alignment ratio of s-polarized direction to p-polarized direction is 1.27 (Fig. 1(c)). Rabi-splitting energy is proportional to the square-root of oscillator strength [1]. Thus, we can estimate the contribution of the alignment is a factor of $\sqrt{1.27} = 1.13$.

Here, we assume that the long axes of J-aggregates are all aligned parallel to the plane of the microcavity by spin-casting. The contribution of this planer alignment is evaluated to be a factor of $1/\cos\theta_c^{\text{res}} = 1.09$. Thus the combined overall contribution of the alignment of J-aggregates is estimated as $1.13 \times 1.09 = 1.23$.

On the other hand, polarization dependence of effective cavity length also affects to the Rabi-splitting energy of a factor of

$$\left(1/\sqrt{L_{\text{eff}}^{\text{calc}(s)}}\right)/\left(1/\sqrt{L_{\text{eff}}^{\text{calc}(p)}}\right) = 1.03.$$

Therefore the ratio of the Rabi-splitting Δ_s/Δ_p is estimated as

$$\Delta_s/\Delta_p = \sqrt{1.27} \times 1/\cos\theta_c^{\text{res}} \times \left(\frac{1/\sqrt{L_{\text{eff}}^{\text{calc}(s)}}}{1/\sqrt{L_{\text{eff}}^{\text{calc}(p)}}}\right) = 1.27.$$

The calculated ratio roughly agrees well with the experimental ratio of $\Delta_s/\Delta_p = 94[\text{meV}]/69[\text{meV}] = 1.36$. The small discrepancy still remains can be implemented such

as surface plasmonic mechanisms in silver mirrors. From these calculations anyhow, we conclude that the strong polarization dependence is mainly due to the alignment of the J-aggregates and that it is not affected so much by a polarization dependence of the penetration depths.

In summary, we fabricated a metal-metal mirror microcavity containing PIC J-aggregates, and measured reflection spectra at various angles for s- and p-polarized incident light, respectively. From the reflection spectra, dispersion relations for upper and lower polaritons are plotted. Large vacuum Rabi-splitting energies, i.e. strong coupling between light and matter, are observed, and the energies are estimated as 94 meV and 69 meV for s- and p-polarized light, respectively. Based on both the experimental results and numerical calculation of penetration depth of light into metallic mirror, it is concluded that the large Rabi-splitting energies are due to not only large oscillator strength of the PIC J-aggregates but also strong confinement of light by the metallic mirror cavity. As for the strong polarization dependence of the Rabi-splitting energies, we described quantitatively that it is mainly due to an alignment of the J-aggregates in the microcavity.

Acknowledgements This research is partly supported by Iketani science and technology foundation.

References

- [1] M. S. Skolnick, T. A. Fisher, and D. M. Whittaker, *Semicond. Sci. Technol.* **13**, 645 (1998).
- [2] P. G. Savvidis, J. J. Baumberg, R. M. Stevenson, M. Skolnick, D. M. Whittaker, and J. S. Roberts, *Phys. Rev. Lett.* **84**, 1547 (2002).
- [3] D. G. Lidzey, D. D. C. Bradley, M. S. Skolnick, T. Virgili, S. Walker, and D. M. Whittaker, *Nature* **395**, 53 (1998).
- [4] J. R. Tischler, M. S. Bradley, V. Bulovic, J. H. Song, and A. Nurmikko, *Phys. Rev. Lett.* **95**, 036401 (2005).
- [5] L. G. Connolly, D. G. Lidzey, R. Butté, A. M. Adawi, D. M. Whittaker, M. S. Skolnick, and R. Airey, *Appl. Phys. Lett.* **83**, 5377 (2003).
- [6] P. A. Hobson, W. L. Barnes, D. G. Lidzey, G. A. Gehring, D. M. Whittaker, M. S. Skolnick, and S. Walker, *Appl. Phys. Lett.* **81**, 3519 (2002).
- [7] T. Tani, M. Oda, T. Hayashi, H. Ohno and K. Hirata, *J. Lumin.*, **122-123**, 244 (2007).
- [8] M. Kasha, *radiat. Res.*, **20**, 55 (1963).
- [9] A. Eisfeld, R. Kniprath, and J. S. Briggs, *J. Chem. Phys.* **126**, 104904 (2007).
- [10] D. G. Lidzey, A. M. Fox, M. D. Rahn, and M. S. Skolnick, V. M. Agranovich, S. Walker, *Phys. Rev.* **B65**, 195312 (2002).
- [11] G. Panzarini, L. C. Andreani, A. Armitage, D. Baxter, M. S. Skolnick, V. N. Astratov, J. S. Roberts, A. V. Kavokin, M. R. Vladimirova, and M. A. Kaliteevski, *Phys. Rev.* **B59**, 5082 (1999).